THE JOURNAL OF PHYSICAL CHEMISTRY B

Article

pubs.acs.org/JPCB

Synthesis and Photophysical Properties of Two Diazaporphyrin–Porphyrin Hetero Dimers in Polar and Nonpolar Solutions

Fawzi Abou-Chahine,[†] Daisuke Fujii,[‡] Hiroshi Imahori,[‡,§] Haruyuki Nakano,[∥] Nikolai V. Tkachenko,[†] Yoshihiro Matano,*[,⊥] and Helge Lemmetyinen*[,†]

[†]Department of Chemistry and Bioengineering, Tampere University of Technology, P.O. Box 540, 33101 Tampere, Finland

[‡]Department of Molecular Engineering, Graduate School of Engineering and [§]Institute for Integrated Cell-Material Sciences (WPI-iCeMS), Kyoto University, Nishikyo-ku, Kyoto 615-8510, Japan

[∥]Department of Chemistry, Graduate School of Sciences, Kyushu University, Fukuoka 812-8581, Japan

[⊥]Department of Chemistry, Faculty of Science, Niigata University, Niigata 950-2181, Japan

Supporting Information

ABSTRACT: Two diazaporphyrin (DAP)-porphyrin hetero dimers, in *β*–*meso* and *β*–*β* configurations, were prepared to study their photoinduced intramolecular electron transfer properties. The two *meso* nitrogen atoms in the porphyrin ring of DAP change its redox potential, making DAP more easily reduced, compared to its porphyrin counterpart. A charge-transfer from porphyrin to DAP in both hetero dimers was verified by versatile optical spectroscopic methods. The steady-state fluorescence spectra indicated an efficient intramolecular exciplex formation for both dimers. For the *β*–*meso* dimer, ultrafast time-resolved spectroscopic methods revealed the subpicosecond formation of two types of primary short-living (1–18 ps) intramolecular exciplexes, which relaxed in toluene to form a long-living final exciplex (1.4 ns) followed by a longer-living charge transfer complex (>5 ns). However, in benzonitrile, the lifetime of the final exciplex was longer (660 ps) as was that of the charge transfer complex (180 ps). The *β*–*β* analogue formed similar short-living exciplexes in both solvents, but the final exciplex and the charge transfer state had significantly shorter lifetimes. The electrochemical redox potential measurements and density functional theory calculations supported the proposed mechanism.

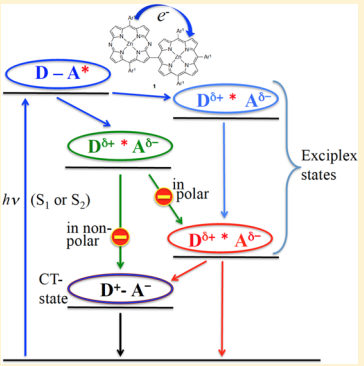

INTRODUCTION

Porphyrin-based multichromophoric compounds are an attractive platform to design new photoactive systems with a multitude of interesting properties and potential applications, from light harvesting in a wide spectral range[1] to fast and efficient photoinduced charge separation.[2] One particularly interesting and challenging approach in designing such compounds involves engineering the electronic coupling between two or more chromophores, which opens up the possibility to tune electronic absorption and emission properties, and to control the efficiency and degree of photoinduced charge separation. It has been shown that at close proximity two covalently linked chromophores may form an intramolecular exciplex, which may be observed as a new broad red-shifted emission band, but more importantly it can be designed as an intermediate state accelerating the formation of a radical ion pair, or a complete charge separated state.[3−5] This raises the importance of studying and understanding the design principles and photophysics of dichromophoric systems with exciplex-like characters.

Photochemical phenomena in porphyrins have been well studied and, to a lesser extent, investigations on the optical properties of diazaporphyrins have also been conducted. 5,15-Diazaporphyrins (DAPs) are a class of porphyrins that bear two *meso*-nitrogen atoms linking two dipyrromethene units. DAPs continue to receive interest in relation to their analogues, porphyrins and phthalocyanines.[6−11] It is well-known that Q bands of DAPs are red-shifted and intensified compared to those of porphyrins. This is because the incorporation of two *meso* nitrogen atoms reduces the molecular symmetry from D_{4h} (porphyrin) to D_{2h} (DAP). In the D_{2h}-symmetric DAP *π*-systems, both the highest occupied molecular orbital (HOMO)/HOMO−1 and lowest unoccupied molecular orbital (LUMO)/LUMO+1 are nondegenerated. In addition, the HOMO and LUMO energies of DAPs are lower than those of their porphyrin counterparts.

Quite recently, we have successfully prepared the first examples of covalently linked DAP dimers by using palladium-catalyzed cross-coupling reactions.[12,13] These DAP dimers have shown variable properties depending on the linkage modes. Among them, the *β*–*β* directly linked DAP dimers have been found to possess coplanar and extended *π*-systems and show

Special Issue: John R. Miller and Marshall D. Newton Festschrift

Received: October 30, 2014
Revised: January 13, 2015
Published: January 15, 2015

DOI: 10.1021/jp510903a
J. Phys. Chem. B 2015, 119, 7328–7337

Scheme 1. Synthesis of Covalently Linked DAP−Porphyrin Hetero Dimers 1 and 2[a]

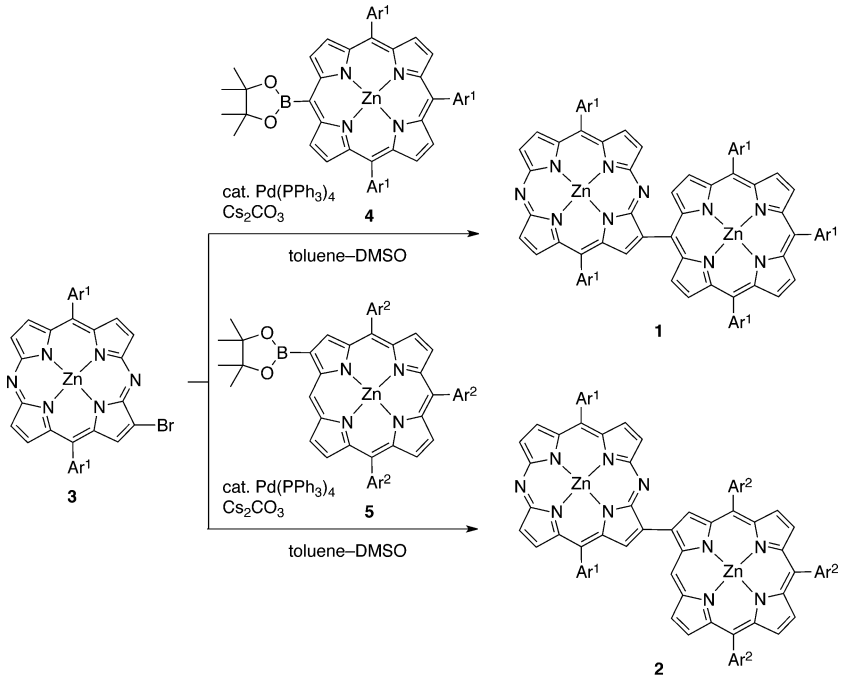

[a]Ar^1 = 2,4,6-$Me_3C_6H_2$. Ar^2 = 3,5-$(t\text{-Bu})_2C_6H_3$.

red-shifted Q bands attributable to the $\pi-\pi^*$ HOMO−LUMO transitions.

The redox properties of DAP are also altered relative to porphyrin, and this can be used to tune the rate and efficiency of the electron transfer, for example when complexed with a fullerene acceptor in a dyad.[14] Owing to the electron-withdrawing character of the 5,15-azasubstitution, DAP is easier to reduce than porphyrin.[8,9] Thus, an electron transfer from porphyrin to DAP would be expected.

Dimers, in which porphyrin (P) is complexed with DAP has not yet been studied. In this work we have synthesized two P-DAP dimers, in which P and DAP are linked with a short single bond linker with different attachment points, providing a $\beta-\beta$ and a $\beta-meso$ configuration. Transient absorption and fluorescence spectroscopy were carried out in two different solvents, toluene and benzonitrile, for both dyads. For each compound, the photophysics was basically the same. Initial formations of two excited dimers were confirmed by ultrafast spectroscopic studies. The more polar solvent, benzonitrile, allowed one excited dimer to relax fast to a charge separated state, while in toluene both excited states relaxed to a third excited dimer, to a significantly longer-living intramolecular exciplex.

Through the observed differences in the photophysics and density functional theory (DFT) calculations it is possible to gather information on the electron density distribution, dependence of the electronic coupling on torsion angle, or the angle between the planes of the chromophore macrocycles. The bonding position in $\beta-meso$ and $\beta-\beta$ configurations greatly influenced the conjugation of electron densities between the dimers and was manifested as retardations of all the photophysical steps of the $\beta-meso$ configuration.

EXPERIMENTAL METHODS

Synthesis of DAP−Porphyrin Hetero Dimers. Scheme 1 summarizes the synthesis of covalently linked DAP−porphyrin dimers **1** and **2**. Suzuki−Miyaura coupling reactions of β-bromo-DAP, **3**, with *meso*-borylporphyrin, **4**,[15] and β-borylporphyrin, **5**,[16] gave $\beta-meso$ linked hetero dimer **1** and $\beta-\beta$ linked hetero dimer **2**, respectively. In the synthesis of **2**, we used compound **5** bearing *meso*-3,5-di(*tert*-butyl)phenyl groups because an analogous β-borylporphyrin bearing *meso*-2,4,6-trimethylphenyl (*meso*-mesityl) groups could not be obtained. However, this difference in substituent groups for the porphyrin moiety of **1** and **2** is not expected to have any profound effect on the physical chemistry of the results described in this article. Figure 1 shows the DAP and porphyrin references, **DAP-ref** and **P-ref** respectively, which were prepared via Suzuki−Miyaura coupling of **3** with mesitylboronic acid and a standard Lindsey condensation of mesitaldehyde with pyrrole,[17] respectively. The hetero dimers **1** and **2**

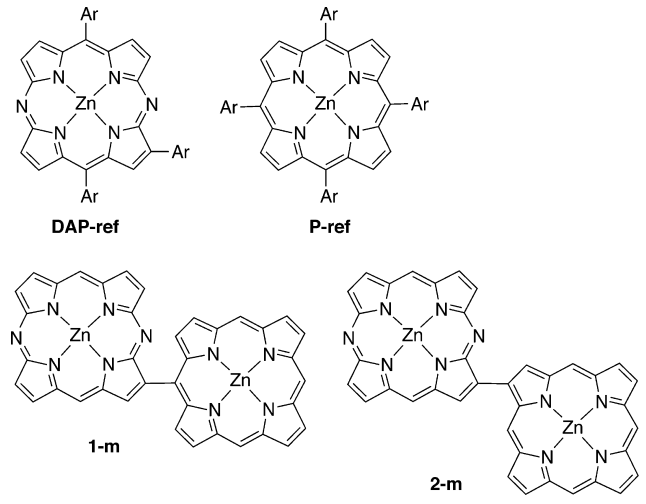

Figure 1. Structures of **DAP-ref**, **P-ref**, **1-m**, and **2-m**. Ar = 2,4,6-$Me_3C_6H_2$.

DOI: 10.1021/jp510903a
J. Phys. Chem. B 2015, 119, 7328−7337

were characterized by ^{1}H NMR spectroscopy and high-resolution mass spectrometry. In the ^{1}H NMR spectrum of **1** in CD_2Cl_2, the DAP-β proton adjacent to the inter-ring bond was observed as a singlet peak at δ 9.51 ppm, whereas, in the ^{1}H NMR spectrum of **2**, the DAP-β, porphyrin-β and *-meso* protons adjacent to the inter-ring bond were observed as singlet peaks at δ 10.93, 10.20, and 9.63 ppm, respectively. The synthesis of **1**, **2** and **DAP-ref** are described in more detail in the Experimental section in the Supporting Information.

Optical Measurements. Steady state absorption spectra were recorded by a Shimadzu UV-3600 spectrophotometer. The steady state emission spectra were measured using a Fluorolog 3 fluorimeter (SpectraACQ), with the excitation wavelength (405 nm) chosen to complement the time-resolved measurements. All spectroscopic measurements were carried out at room temperature and for time-resolved spectroscopy the solutions in the cuvettes were constantly stirred to minimize sample degradation and reduce the probability of exciting the same molecules within the time scale of a spectral acquisition.

Time-Resolved Fluorescence Spectroscopy. Fluorescence decays in the nanosecond time domain were measured using a time-correlated single-photon counting instrument (TCSPC, PicoQuant GmbH), which used a PDL-800-B driver and a PicoHarp-200 controller. A pulsed diode laser (LDH−P-C-405B) excited the samples at 405 nm while the fluorescence decays were typically monitored at the emission band centers, which are 735 and 665 nm for **1** and **2** respectively, regardless of solvent. The full-width half-maximum (fwhm) time resolution of the TCSPC measurements was ca. 65 ps.

Ultrafast fluorescence decays were measured using an up-conversion method described elsewhere,[18] with a temporal resolution of ∼150 fs. In brief, fundamental pulses of 810 nm produced by a Ti:sapphire laser (TiF50, CDP-Avesta) at 80 MHz repetition rate were split into two beam. One portion underwent second harmonic generation to excite the sample at 405 nm, generating emission. The second portion of the fundamental pulse beam was passed to a delay line and then mixed with the emission to achieve frequency up-conversion. The resulting UV photons were detected by a photon counting photomultiplier coupled with a monochromator with a typical averaging of 10 s at each delay time.

Pump Probe Spectroscopy. For transient absorption measurements, a subpicosecond resolution setup was used and described in detail elsewhere.[19] Briefly, 800 nm laser pulses at a 1 kHz repetition rate were generated by a Ti:sapphire laser system (Libra F, Coherent Inc.). The fundamental pulses were split into two beams: one pump beam was guided through an optical parametric amplifier (Topas C, LightConversion Ltd.) to generate the excitation pulses at 380 nm. The pump beam and the rest of fundamental were delivered to a pump−probe measurement system (ExciPro, CDP Inc.). The system generated a white light continuum (WLC) from the 800 nm beam which was used as a probe pulse. The probe was guided through a delay line with a moving right angle reflector that changed the optical path length of the probe with respect to the pump beam. The maximum time scale available to monitor absorption changes was ca. 6 ns. The probe pulse was split in two to obtain signal and reference beams that both passed through the sample. The signal beam was overlapped with the pump beam, while the reference beam was not. The excitation was modulated by a chopper synchronized with excitation pulses to detect probe pulse spectra with and without excitation and to calculate the differential transient absorbance for each excitation pulse. Measurements were recorded with a 10 s average for each delay time, i.e., averaging 10000 excitation shots. The spectra were acquired in two ranges: 550−750 nm and 850−1070 nm. The measurements around the fundamental wavelength, 800 nm, were unreliable since the continuum was very uneven close to the fundamental.

The raw data were fit globally by a sum of exponents to perform data analysis, a procedure that has been described in more detail previously.[18] Briefly, the number of exponents needed for a reasonable fit quality yielded the number of transient species in the photoinduced processes. The rate constants for the formation or relaxation of transient species can be calculated from the respective lifetimes of each component. The results of the fits are presented as decay component spectra with the amplitudes of the exponents plotted as functions of wavelength. A decay component spectrum describes the amplitudes, or intensities, of each individual function representing each lifetime in the sum function, as the function of wavelength. A negative amplitude for any component implies a negative pre-exponential factor in the exponential fit and thus the formation of a transient species within the lifetime of its decay. A positive pre-exponential factor implies the decay of the transient species.

Quantum Chemical Calculations. The geometries of **1-m** and **2-m** were optimized using the DFT method. The basis sets used were 6-311G(d,p) basis set[20] for H, C, and N and the Wachters-Hay all electron basis set[21−23] supplemented with one f-function (exponent: 1.62) for Zn. The functional of DFT was the Becke, three-parameter, Lee−Yang−Parr (B3LYP) exchange-correlation functional.[24,25] We confirmed that the optimized geometries were not on a saddle point. The Cartesian coordinates are summarized in Table S1. All the calculations were carried out using the Gaussian 09 suite of programs.[26]

RESULTS

Structures. To obtain deeper insight into the structures of **1** and **2**, we performed DFT calculations of their model compounds **1-m** and **2-m**, shown in Figure 1, at the B3LYP/6-311G(d,p) level. The optimized structures, selected Kohn−Sham molecular orbitals (MOs), and orbital energies of **1-m** and **2-m** are summarized in Figure 2.

In these hetero dimer models, the DAP and porphyrin rings are twisted with respect to each other, and the torsion angle between the DAP and porphyrin π-planes in **2-m** (30°) is considerably narrower than that in **1-m** (71°). This indicates that the π-conjugation through an inter-ring bond in **2-m** is more effective than that in **1-m** from a geometric point of view. As shown in Figure 2, the HOMO and HOMO−1 reside on the porphyrin unit, whereas the LUMO and LUMO+1 reside on the DAP unit. In addition, the HOMO−2 and HOMO−3 reside on the DAP unit, whereas the LUMO+2 and LUMO+3 on the porphyrin unit. These features are reasonable, considering that the DAP π-system has intrinsically low-lying HOMO/HOMO−1 and LUMO/LUMO+1 compared with the porphyrin π-system.

Redox Potentials. To know the electrochemical properties of the hetero dimers, we measured redox potentials of **1**, **2**, **DAP-ref**, and **P-ref** in tetrahydrofuran (THF) by cyclic voltammetry with nBu$_4$NPF$_6$ as the supporting electrolyte. The voltammograms are shown in Figure S1 in the Supporting Information. The first oxidation potentials ($E_{ox,1}$) of **1** and **2** are

DOI: 10.1021/jp510903a
J. Phys. Chem. B 2015, 119, 7328−7337

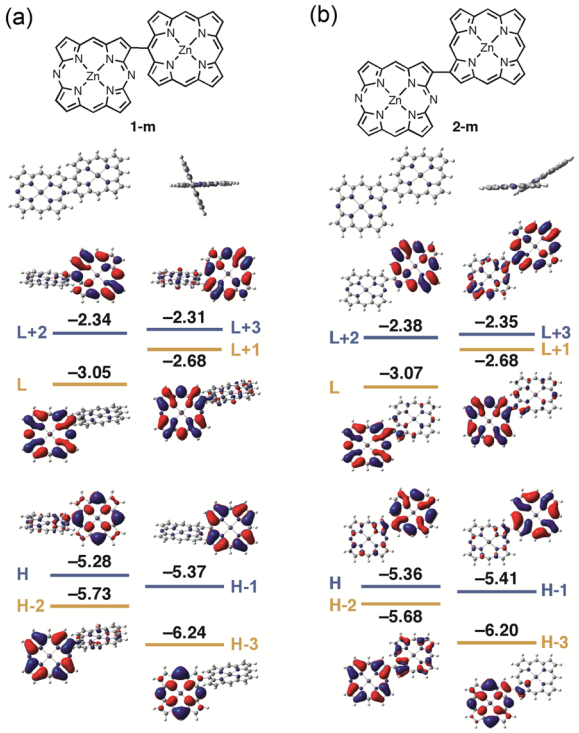

Figure 2. Selected Kohn−Sham molecular orbitals and their energies (in eV) of the optimized structures of (a) **1-m** and (b) **2-m** calculated at the B3LYP/6-31G(d,p) level. H = HOMO; L = LUMO.

+0.33 and +0.36 V, respectively (vs ferrocene/ferrocenium; Fc/Fc$^+$), which are close to the $E_{ox,1}$ value of **P-ref** (+0.36 V) and much more negative than that of **DAP-ref** (+0.73 V). On the other hand, the first reduction potentials ($E_{red,1}$) of **1** and **2** are −1.44 and −1.46 V, respectively (vs Fc/Fc$^+$), which are close to the $E_{red,1}$ value of **DAP-ref** (−1.47 V) and much more positive than that of **P-ref** (−2.07 V). These data are in good agreement with the theoretical predictions, and indicate that the HOMO and LUMO of the hetero dimers essentially possess the characters of the porphyrin and DAP units, respectively. The electrochemical measurements predict for the free energy of the charge separated state, where electron is localized on **DAP** and hole on **Por**, values of 1.77 and 1.82 eV for **1** and **2**, respectively.

Absorption and Emission Properties of *β*−*meso* and *β*−*β* Compounds in Toluene and Benzonitrile. The absorption and emission spectra of the reference compounds **DAP-ref** and **P-ref** in toluene are shown in Figure 3.

Figure 4 compares the absorption and emission bands of the both hetero dimers, **1** and **2**, in toluene and benzonitrile. The emission bands are broad and intense, particularly for those in toluene. The change of the solvent does not alter the ground state absorption bands significantly for either dimer.

The fluorescence quantum yields of the dyads are for the *β*−*meso* compound 0.12 and 0.01 and for the *β*−*β* compound 0.18 and 0.02 in toluene and benzonitrile, respectively.

Photophysical Properties of *β*−*meso* Compound in Toluene and Benzonitrile. Figure 5a shows the transient absorption decay component spectra of the hetero dimer **1** in toluene. It was necessary to employ a four exponential function to obtain a satisfactory fitting.

After exciting the second excited state of the dimer **1** at 380 nm, it first undergoes an S_2−S_1 transition via the internal

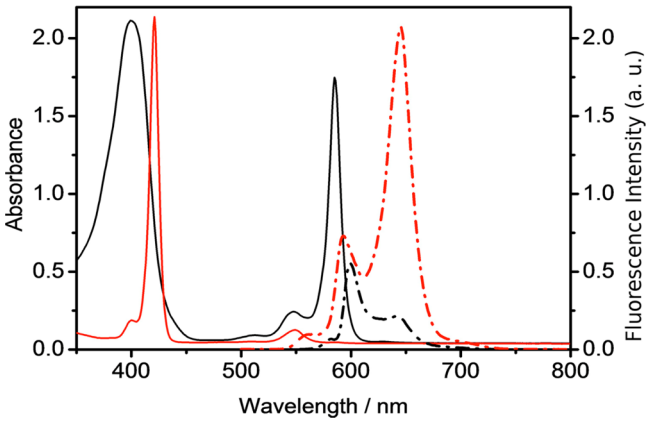

Figure 3. Absorption (solid lines) and emission (dotted lines) spectra of the reference compounds **DAP-ref** (black) and **P-ref** (red) in toluene.

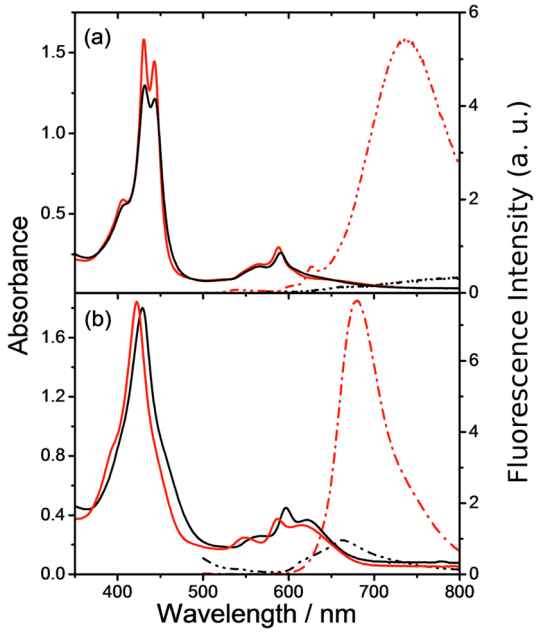

Figure 4. Absorption (solid lines) and emission (dashed lines) spectra for (a) the *β*−*meso* dimer (compound **1**) and (b) the *β*−*β* dimer (compound **2**) in toluene (red) and in benzonitrile (black).

conversion (IC) on a subpicosecond time scale, which is not time-resolved in this measurement. The lifetimes of the two shortest living components are ca. 0.6 and 17 ps, both having two minima. For the 0.6 ps component the minima are at 660 and 1040 nm, and those for the 17 ps component at 710 and 980 nm, as shown in Figure 5a. Both components contribute to the formation of a new common intermediate state with two broad bands, with maxima at 680 and 1000 nm and a lifetime of 1.4 ns. This state decays to form a long-living intermediate with a lifetime longer than the instrumental resolution, > 5 ns.

The same phenomenon can be seen in Figure 5b, which shows the spectral evolution at different time delays. By 3 ps, two positive absorption bands (at 660 and 1030 nm) are formed mainly from the 0.6 ps component. By 500 ps, as the 17 ps component has also decayed, the bands are shifted to 680 and 1000 nm, respectively, and resemble the component spectrum of the 1.4 ns component (Figure 5a).

DOI: 10.1021/jp510903a
J. Phys. Chem. B 2015, 119, 7328−7337

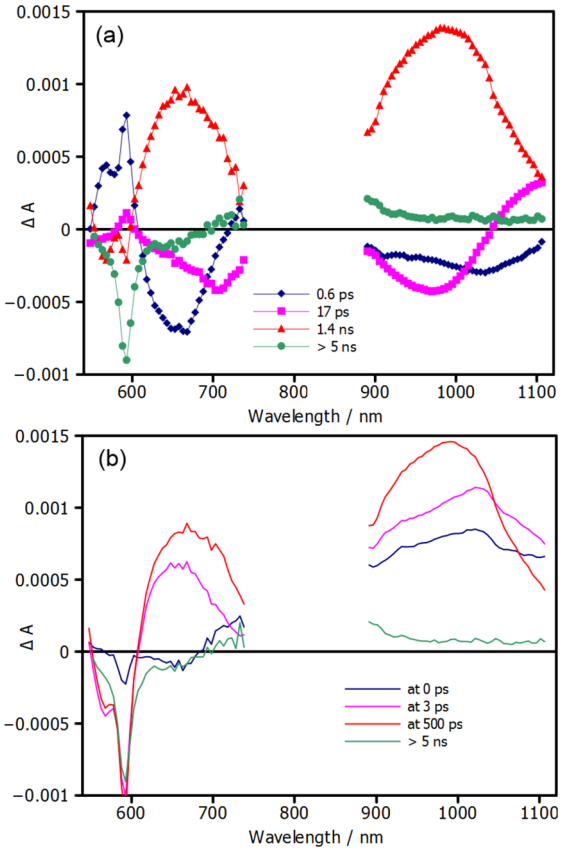

Figure 5. Transient absorption decay component spectra (a) and delay spectra (b) of compound **1** in toluene. The excitation wavelength was 380 nm.

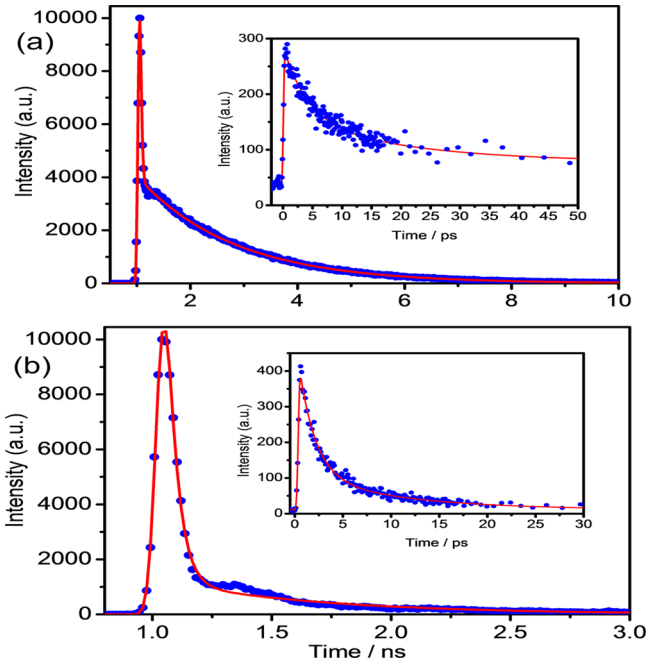

Figure 6. Fluorescence decay profiles for compound **1** (a) in toluene (<4 ps, 20 ps, 1.8 ns) and (b) in benzonitrile (1.7 ps, 10.2 ps, 670 ps). The excitation and monitoring wavelengths are 405 and 750 nm, respectively. The inset graphs show the fluorescence up-conversion measurements. The excitation and monitoring wavelengths are 412 and 700 nm, respectively.

The components of compound **1**, corresponding to those with lifetimes of 0.6 ps, 17 ps, and 1.4 ns in Figure 5a, were also observed in emission decays, measured by the TCSPC and up-conversion methods, and are shown in Figure 6a. Due to a poorer time-resolution, the measured lifetimes are <4 ps, 20 ps, and 1.8 ns, satisfactorily close to those of the pump−probe measurements. It is important that the three shortest living transient absorption components have also emissions.

In addition to the 380 nm excitation (S_2 state of DAP), Figure 5a, the transient absorption spectra of **1** were recorded in toluene also with the excitation wavelengths of 405 nm (S_2 state of DAP, to some extent that of P) and 560 nm (S_1 state of DAP, to some extent that of P), shown in Figures S2 and S3, respectively, in the Supporting Information. It is important to note that exactly the same processes were observed when the Q-band (S_1 state) or the Soret band (S_2 state) of compound **1** were exited in toluene. In benzonitrile, exactly the same independence of the excitation energy was also observed.

The transient lifetimes for compound **1** in toluene were thus determined from four different experiments, namely three series of transient absorption measurements with different excitation wavelengths and one emission decay measurement. The averages of the time constants of the two fastest components are ca. 1 and 18 ps, and both of them were observed by fluorescence and absorption methods. The relaxation of these short-living states leads to the formation of a longer-living intermediate, with an average lifetime of 1.4 ns. These values are used in the following discussion.

The decay component spectra for dimer **1** in benzonitrile are shown in Figure 7. Two components, with lifetimes of 2.4 and

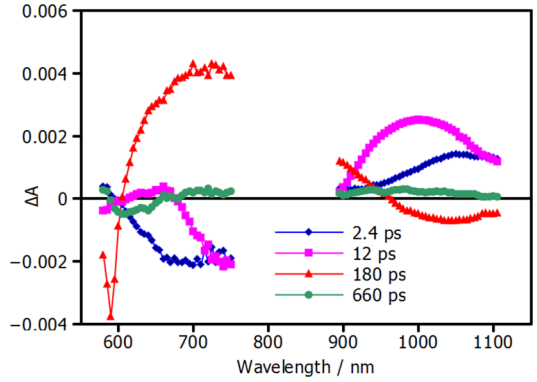

Figure 7. Transient absorption decay component spectra of compound **1** in benzonitrile. The excitation wavelength was 560 nm.

12 ps, have negative amplitudes in the visible region, whose minima are at 680 and 740 nm, respectively. In the near-IR region, however, these two components appear with positive amplitudes at 1040 and 1000 nm, respectively. A broad and strong absorption band from 600 nm to about 800 nm is formed from at least one of the two transient components. This new transient species also has a negative band in the near-IR region and a lifetime of 180 ps. Eventually, a long-living component with a 660 ps lifetime is observed in both the visible and near-IR spectral regions.

Figure 6b shows the emission profiles of compound **1** in benzonitrile at 750 nm on the nanosecond time scale, with the inset showing the emission profile at 700 nm at early times. The 1.7 and 10.2 ps emission lifetimes correspond well to the

DOI: 10.1021/jp510903a
J. Phys. Chem. B 2015, 119, 7328−7337

transient absorption component time constants, 2.4 and 12 ps in Figure 7. The two fluorescent components account for 95% of the emission intensity, and the remaining much slower component (670 ps) only 5%. This lifetime corresponds perfectly with the transient absorption component with the lifetime of 660 ps. Due to the very low signal intensity, the emission at 700 nm could not be measured in the nanosecond time scale by the fluorescence up-conversion method.

Photophysical Properties of *β*–*β* Compound in Toluene and Benzonitrile. Figure 8 shows the transient absorption decay component spectra of dimer **2** in toluene. There is a fast 0.3 ps signal, a decay (a positive signal) and formation in the visible and near-IR regions, respectively. The lifetime could correspond to the decay time of the singlet excited state, but this state has no absorption at the near-IR. Thus, it is just a short-living state formed very fast. Another, a 9 ps component is also seen in the visible range. From those two transient states, a long-living species is formed, with a lifetime of 600 ps, which gives rise to a broad absorption band in the near-IR and a narrower one in the visible region. This new species decays to form a state with lifetime of about 6 ns, which can be seen as bleaching of the ground state absorption at 570–670 nm.

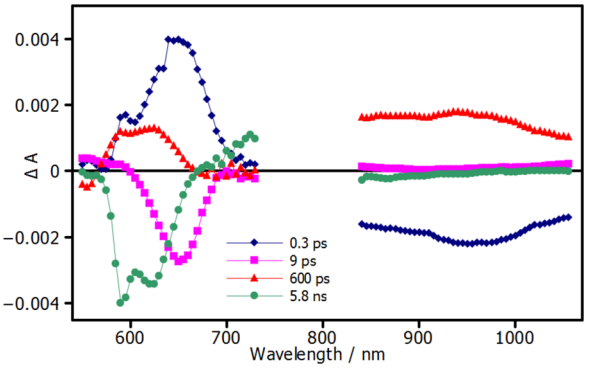

Figure 8. Transient decay component spectra of compound **2** in toluene. The excitation wavelength was 380 nm.

Figures 9 and 10 show the transient absorption decay component spectra and the emission decay, respectively, for dimer **2** in benzonitrile. The transient absorption dynamics have similarities with its *β*–*meso* analogue, **1**, in benzonitrile. A fast formation of a transient absorption signal (0.75 ps) is accompanied by a short-lived transient species with a lifetime of 8.5 ps, which has a negative amplitude at 750 nm and a positive amplitude at 1100 nm. A broad absorption band from the visible to the near-IR grows when the preceding transients decay. This has a lifetime of 83 ps. A weak transient band with a lifetime close to 900 ps still remains.

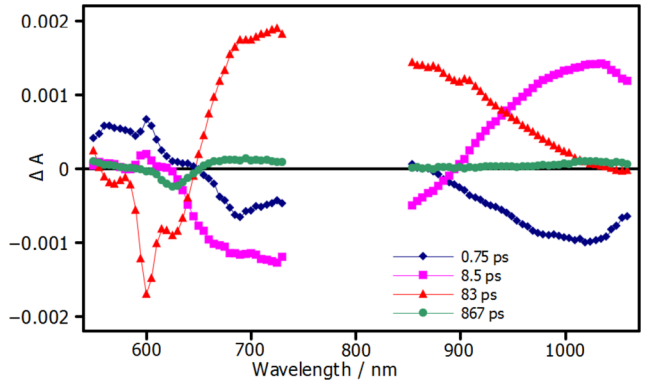

Figure 9. Transient decay component spectra of compound **2** in benzonitrile. The excitation wavelength was 380 nm.

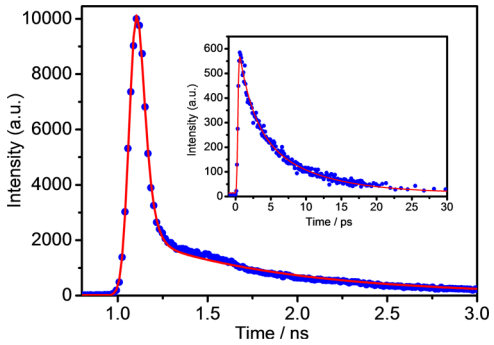

Figure 10. Fluorescence decay profiles for compound **2** in benzonitrile (0.9 ps, 8.1 ps, 860 ps). The excitation and monitoring wavelengths are 405 and 655 nm, respectively. The inset graph shows the fluorescence up-conversion measurement. The excitation and monitoring wavelengths are 432 and 655 nm, respectively.

The time-resolved emission profiles of **2** in benzonitrile are shown in Figure 10. At least 90% of the emission occurs within 100 ps, while the lifetime of the remaining slow relaxation is determined to be 860 ps, which is complementary to the low intensity transient component in Figure 9. The up-conversion emission decay was fitted to two components of 0.9 (50%) and 8.1 ps (50%), which similarly complement the transient absorption decay components.

DISCUSSION

General. There are a few general characteristic properties common for both hetero dimers investigated, as well as the effect of the different solvents on their physical behavior. First, the fluorescence emissions of the both dimers are not the superposition of the sum of the fluorescence of their monomers. Instead, the dimers have significantly red-shifted, broad, and structureless emission bands, typical for excited emitting molecular dimers, known as excimers or exciplexes. The emission in the more polar environment, benzonitrile, is less intensive than in the almost nonpolar toluene. This phenomenon is well-known for dimers forming charge transfer complexes.[18] It should be noted that the chromophoric moieties of the dimer increase the intramolecular conjugation length. The two chromophoric rings are twisted with respect to each other at the optimized structures of **1-m** and **2-m** in the ground state (Figure 2). Although we have not optimized the excited-state structures, the twisted conformations of **1-m** and **2-m** may suggest that the two chromophores can rotate rapidly about the inter-ring bond to more conjugated conformers in the excited states.

Based on the steady-state optical properties of the studied monomers and dimers, we propose the photoinduced processes described in Scheme 2. The initial excitation pulse forms an excited singlet state, either directly or via an IC process from the second excited state, in a dimer denoted as P*-DAP or P-DAP*. This state may relax back to the ground state via fluorescence, with a rate constant of k_F. More likely, however, is that the excited dimer forms an intramolecular exciplex (P-DAP)*, with a rate constant of k_{exp}. This exciplex may form a

DOI: 10.1021/jp510903a
J. Phys. Chem. B 2015, 119, 7328–7337

Scheme 2. An Initial Hypothesis for the Reaction Scheme for the Relaxation Pathways of the Excited State of Dimers 1 and 2

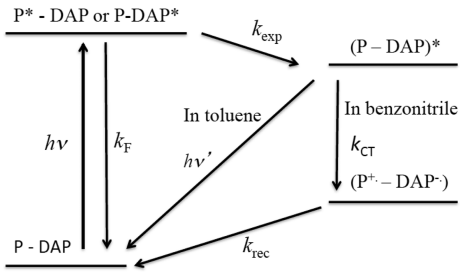

single or triplet charge separated state, ($P^{+\bullet}$–$DAP^{-\bullet}$), which is favored in the more polar environment such as benzonitrile. Alternatively, the exciplex may relax to the ground state in either a radiative or nonradiative transition. In the case of a charge separated state (CSS), a recombination of the charges via back electron transfer relaxes the transient species back to the ground state with a rate constant of k_{rec}.

The time-resolved pump–probe and emission measurements yielded, however, more complex, but simultaneously more detailed information on the processes involved. The most remarkable observation is that, instead of two transient species (Scheme 2), four transient species were detected for both dimers and in both solvents; three of those were emissive, instead of the one supposed in Scheme 2.

Based on the steady-state fluorescence results the long-living fluorescent components (1.4 and 0.66 ns for compound **1** and 0.60 and 0.87 ns for compound **2** in toluene and benzonitrile, respectively) are intramolecular exciplexes formed in excitation of the dyads. They were preceded by two short-living transient species, which were formed in time shorter than 100 fs directly from two different ground state conformers, in which the chromophores are twisted with respect to each other. The formed excited complexes both show fluorescence at lower energy than neither of the parent moieties. This is a general property of exciplexes and justifies assignment of those two species to *primary exciplexes*.

Because the primary exciplexes are formed directly from their ground state conformers, their energies are not optimized to the minumum of each excited dimer. As soon as a primary exciplex is formed it relaxes rapidly, in few picoseconds to few tens of picoseconds, by rotation about the inter-ring bond to a conformer corresponding to the minimum energy in the excited state, forming the *final exciplex*, which could be common for both primary exciplexes. Alternatively, a primary exciplex could relax to another transient species, e.g., to a charge transfer (CT) state.

Another general observation was that different excitation wavelengths did not result in distinguishable difference in transient absorption responses. This means that (1) involvement of the second excited state of either of the excited chromophores does not play any essential role in the electron transfer reaction, instead (2) the internal conversion from the second to the first singlet excited state of porphyrin or diazaporphyrin, S_2–S_1, is fast and not time-resolved, and (3) the formations of the excited complexes are also fast and do not depend on the primary excited chromophore.

Compounds 1 and 2 in Toluene. According to the ultrafast pump–probe experiments, exciting compound **1** in toluene resulted in the formation of two short-lived transient species with average time constants of 1 and 18 ps (Figures 5, S2, and S3). These components were also determined by the fluorescent up-conversion method (Figure 6a) and are considered as primary exciplexes of compound **1**. The relaxation of these two states led to the formation of a relative long-living intermediate, with an average lifetime of 1.4 ns. This lifetime was also measured for the decay of the broad emission band assigned to an exciplex. This exciplex relaxes to a long-living, > 5 ns, nonemitting state, which is probably a CT state, ($P^{+\bullet}$-$DAP^{-\bullet}$).

Similarly, when compound **2** was excited in toluene, two primary exciplexes were formed very quickly and decay to the final exciplex with lifetimes of 0.3 and 9.0 ps (Figure 8). The final exciplex lives 600 ps and forms a CT state, which decays with a lifetime of 5.8 ns. These processes mirror the observations for compound **1** in toluene, but are significantly faster. The implication is that the difference in geometry and π-conjugation between the two dimers results in a faster relaxation of the excited states in **2**.

In summary, compounds **1** and **2** can exist as two different conformers in the ground state, which form under light excitation two primary intramolecular exciplexes. The photo-induced processes for compounds **1** and **2** are shown in Scheme 3, with the experimental rate parameters being related

Scheme 3. Proposed Reaction Scheme and Kinetics for the Relaxation Pathways of the Excited Singlet State of Dimer 1 in Toluene

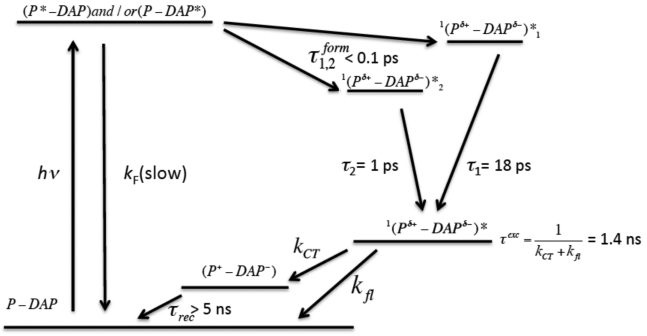

to compound **1**. The lifetime of the longer-living primary exciplex is marked by τ_1 = 18 ps and that of the shorter-living exciplex by τ_2 = 1 ps. This selection will be justified later. The lifetimes are summarized in Table 1.

According to Scheme 3, excitation of either the porphyrin or the diazaporphyrin moiety leads to formation of the two very short-living exciplexes ^{1}(P-DAP)$_1$* and ^{1}(P-DAP)$_2$*. These transient species transform to the final exciplex, ^{1}(P-DAP)*, which, like the primary exciplexes, also have some charge

Table 1. Lifetimes of the Transient States of Compounds 1 and 2 in Toluene and Benzonitrile[a]

		τ_1 (ps)	τ_2 (ps)	τ^{exc} (ns)	τ_{rec} (ns)
1	toluene	1	18	1.4	>5
	benzonitrile	2.4	12	0.66	0.185
2	toluene	0.3	9.0	0.60	5.85
	benzonitrile	0.9	8.5	0.87	0.08

[a] τ_1 and τ_2 are the lifetimes of the emissive primary transient states, τ^{exc} is the lifetime of the exciplex, and τ_{rec} is the recombination time of the CT state. See Schemes 3 and 4.

DOI: 10.1021/jp510903a
J. Phys. Chem. B 2015, 119, 7328–7337

transfer character due to the differences in their electron donor−acceptor properties. The final exciplex relaxes to a charge transfer complex, which recombines back to the ground state.

Compounds 1 and 2 in Benzonitrile. Exciting compounds **1** and **2** in benzonitrile resulted in the formation of two short-living transient species for both conformers, with averaged time constants of 2.4 and 12 ps for compound **1** (Figures 6b and 7) and 0.9 and 8.5 ps for compound **2** (Figures 9 and 10). They are considered as primary exciplexes of compounds **1** and **2** in benzonitrile. The third emitting state, the final exciplex, has a lifetime of 660 or 870 ps for compounds **1** and **2**, respectively.

There are, however, two important differences between the optical and photophysical properties of compound **1** and **2** in toluene and benzonitrile. First, the fluorescence quantum yields, mainly due to the exciplex emissions, are 12 and 8 times higher in toluene than in benzonitrile for compound **1** and **2**, respectively. Second, as the longest living component in toluene for both compounds was observed to be the charge transfer complex, ($P^{+\bullet}$-$DAP^{-\bullet}$), with lifetimes >5 ns, longer than the exciplex fluorescence lifetimes (1.4 and 0.60 ns, for **1** and **2**), in benzonitrile the longest living component was the transient exciplex with lifetimes of 660 ps for compound **1** (Figures 6b and 7) and 870 ps for compound **2** (Figures 9 and 10). In the pump probe experiments, however, shorter living (180 and 83 ps, for **1** and **2**, respectively) nonemitting intermediate states were observed (Figures 7 and 9). They could not be formed from the longer-living exciplex.

Nevertheless, the apparent difference in the solvent-dependent behavior is simple to resolve, if either of the primary short-living exciplexes, ^{1}(P-DAP)$_1$* or ^{1}(P-DAP)$_2$* would relax directly to the charge transfer complex, ($P^{+\bullet}$-$DAP^{-\bullet}$), as shown in Scheme 4 for compound **1** in benzonitrile. The CT state

Scheme 4. Proposed Reaction Scheme and Kinetics for the Relaxation Pathways of the Excited Singlet State of Dimer 1 in Benzonitrile

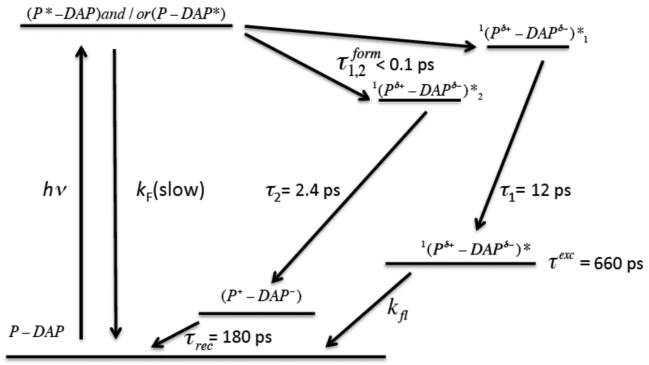

decays with the recombination time of τ_{rec} = 180 ps. In Scheme 4 the shorter-living primary exciplex, ^{1}(P-DAP)$_2$*, decays to charge transfer complex, with a time constant of τ_2 = 2.4 ps. This will be justified below.

Solvent-Dependent Behavior. Because the fluorescence quantum yield of compound **1** is 12 times lower in benzonitrile, it is logical to suppose that the shorter-living primary exciplex, ^{1}(P-DAP)$_2$*, with lifetime of τ_2 = 2.4 ps, would relax to the charger transfer complex, and thus reduce the fluorescence quantum yield. If one supposes the formation efficiencies of the primary exciplexes to be equal, 0.5 for both, the quantum yields for the formation of the final exciplex state, $^1(P^{\delta+}\text{-}DAP^{\delta-})^*$, would be in benzonitrile

$$\Phi_{BN}^{exc} = 0.5 \times \frac{1/\tau_1}{(1/\tau_1 + 1/\tau_2)} = 0.5 \times 0.165 = 0.083$$

and in toluene

$$\Phi_{Tol}^{exc} = 0.5 \times 1 = 0.5$$

Furthermore, the total fluorescence quantum yields for the final exciplex state would be in benzonitrile (Scheme 4)

$$\Phi_{BN}^{fl} = \Phi_{BN}^{exc} \times \frac{k'_{fl}}{k'_{fl} + k_{nr}} = \Phi_{BN}^{exc} \times k'_{fl}\tau_{BN}^{exc}$$

where k'_{fl} and k_{nr} (not shown in Scheme 4) are the radiative and nonradiative rate constants, respectively, of the exciplex state.

Analogously, in toluene (Scheme 3),

$$\Phi_{Tol}^{fl} = \Phi_{Tol}^{exc} \times \frac{k''_{fl}}{k''_{fl} + k_{CT}} = \Phi_{Tol}^{exc} \times k''_{fl}\tau_{Tol}^{exc}$$

The ratio of the fluorescence quantum yields in toluene and benzonitrile is

$$\frac{\Phi_{Tol}^{fl}}{\Phi_{BN}^{fl}} = \frac{\Phi_{Tol}^{exc} \times k''_{fl}\tau_{Tol}^{exc}}{\Phi_{BN}^{exc} \times k''_{fl}\tau_{BN}^{exc}} = \frac{0.5 \times k''_{fl} \times 1.4\ \text{ns}}{0.083 \times k'_{fl} \times 0.66\ \text{ns}} = 12.8 \times \frac{k''_{fl}}{k'_{fl}}$$

when the experimental rate parameters shown in Schemes 3 and 4 are applied. The ratio is very close to the experimental quantum yield ratio, 12, if the ratio of the radiative rate constants in benzonitrile and toluene is $k''_{fl}/k'_{fl} \approx 1$. Analogical treatment could be done for compound **2**. The time constants related to Scheme 4 for both compounds are combined in Table 1.

The main reason for the reduced fluorescence efficiency of compound **1** in benzonitrile is the fast decay of the short living primary exciplex to the CT state, ($P^{+\bullet}$-$DAP^{-\bullet}$). This is strongly supported by comparison of the transient absorption decay component spectra in Figures 7 and S3, in which compound **1** is excited at 560 nm. In benzonitrile (Figure 7) the most intense transient (at 720 nm) is the CT state with lifetime of 180 ps. In toluene (Figure S3) the most intense component is the exciplex state (maxima at 660 and 990 nm), with lifetime of 1.2 ns, whereas the intensity of the CT state (at 720 nm) is relative low. Similarly, in transient absorption decay component spectra for compound **2**, as it was for compound **1**, the most intense transient in benzonitrile (Figure 9) is the CT state with lifetime of 83 ps. In toluene (Figure 8), the most intense component is the exciplex state with lifetime of 600 ps.

Almost all the transient components for dimer **2** relax faster than those formed in dimer **1**, regardless of solvent. These observations are complementary to the greater π-conjugation in dimer **2** determined computationally. However, it is clear that the lifetime of the final exciplex for dimer **2** in benzonitrile is slightly longer than for dimer **1**. Although this contradicts the previous observations, there are two potential explanations. First, the difference is small and within the error of the measurements. Alternatively, the energy of the final exciplex in dimer **2** is slightly lower than its counterpart in compound **1**. This might lead to a more stable exciplex that would manifest itself as a longer-lived one. The lifetimes of the transient states for compounds **1** and **2** in toluene and benzonitrile are presented in Table 1.

DOI: 10.1021/jp510903a
J. Phys. Chem. B 2015, 119, 7328−7337

CONCLUSIONS

This study shows that after photoexcitation of the *β−meso* and *β−β* dimers of the diazaporphyrin (DAP)-porphyrin dyad in nonpolar toluene, both form a relatively long-living intramolecular exciplex, which has a strong emission and relaxes first to a charge transfer complex, and then recombines to the ground state. For both dimers the long-living exciplex is preceded by two short living primary transient states, observed by the ultrafast pump−probe method and as two fluorescent species by the fluorescence up-conversion method. Because the two chromophoric rings of the hetero dimers are twisted with respect to each other, they might be able to rotate rapidly about the inter-ring bond in the excited state. This would explain the nature of the two observed exciplex type transients, before the formation of the long-living exciplex. In a more polar environment like benzonitrile, the shorter-living primary exciplexes relax, however, directly to the charge transfer complex, which has a shorter lifetime than the observed excimer emission. The electrochemical redox potential measurements and DFT calculations support the proposed mechanism.

ASSOCIATED CONTENT

Supporting Information

The following data are provided: (i) Voltammograms for compounds **1**, **2**, **DAP-ref**, and **P-ref**, (ii) transient decay component spectra of compound **1** in toluene at the excitation wavelengths of 405 and 560 nm, (iii) experimental and spectroscopic information on the synthesis of compounds **1**, **2**, **DAP-ref** and **P-ref**, (iv) the Cartesian coordinates of the optimized geometries of **1-m** and **2-m**, (v) a full list of the authors of Gaussian 09, Revision B.01, and (vi) author information. This material is available free of charge via the Internet at http://pubs.acs.org..

AUTHOR INFORMATION

Notes

The authors declare no competing financial interest.

ACKNOWLEDGMENTS

H.L. acknowledges the financial support from the Academy of Finland (UVIADEM) and the Finnish Funding Agency for Technology and Innovation (Biosphere). N.V.T. acknowledges the financial support from the Academy of Finland (Photonic QCA). Y.M. acknowledges the financial supports from JSPS KAKENHI Grant Number 25109524 and the Nagase Foundation.

REFERENCES

(1) Kim, D.; Osuka, A. Directly Linked Porphyrin Arrays with Tunable Excitonic Interactions. *Acc. Chem. Res.* **2004**, *37*, 735−745.

(2) Gust, D.; Moore, T. A.; Moore, A. L. Solar Fuels via Artificial Photosynthesis. *Acc. Chem. Res.* **2009**, *42*, 1890−1898.

(3) Mataga, N.; Taniguchi, S.; Chosrowjan, H.; Osuka, A.; Yoshida, N. Ultrafast Charge Transfer and Radiationless Relaxations from Higher Excited State (S2) of Directly Linked Zn-Porphyrin (ZP)-Acceptor Dyads: Investigations into Fundamental Problems of Exciplex Chemistry. *Chem. Phys.* **2003**, *295*, 215−228.

(4) Mataga, N.; Chosrowjan, H.; Taniguchi, S. Ultrafast Charge Transfer in Excited Electronic States and Investigations into Fundamental Problems of Exciplex Chemistry: Our Early Studies and Recent Developments. *J. Photochem. Photobiol. C Photochem. Rev.* **2005**, *6*, 37−79.

(5) Lemmetyinen, H.; Tkachenko, N. V.; Efimov, A.; Niemi, M. Photoinduced Intra- and Intermolecular Electron Transfer in Solutions and in Solid Organized Molecular Assemblies. *Phys. Chem. Chem. Phys.* **2011**, *13*, 397−412.

(6) Ogata, H.; Fukuda, T.; Nakai, K.; Fujimura, Y.; Neya, S.; Stuzhin, P. A.; Kobayashi, N. Absorption, Magnetic Circular Dichroism, IR Spectra, Electrochemistry, and Molecular Orbital Calculations of Monoaza- and Opposite Diazaporphyrins. *Eur. J. Inorg. Chem.* **2004**, *2004*, 1621−1629.

(7) Pan, N.; Bian, Y.; Yokoyama, M.; Li, R.; Fukuda, T.; Neya, S.; Jiang, J.; Kobayashi, N. Sandwich-Type Heteroleptic Opposite -(Diazaporphyrinato)cerium Complexes: Synthesis, Spectroscopy, Structure, and Electrochemistry. *Eur. J. Inorg. Chem.* **2008**, *2008*, 5519−5523.

(8) Matano, Y.; Shibano, T.; Nakano, H.; Kimura, Y.; Imahori, H. Free Base and Metal Complexes of 5,15-Diaza-10,20-Dimesitylporphyrins: Synthesis, Structures, Optical and Electrochemical Properties, and Aromaticities. *Inorg. Chem.* **2012**, *51*, 12879−12890.

(9) Matano, Y.; Shibano, T.; Nakano, H.; Imahori, H. Nickel(II) and Copper(II) Complexes of B-Unsubstituted 5,15-Diazaporphyrins and Pyridazine-Fused Diazacorrinoids: Metal-Template Syntheses and Peripheral Functionalizations. *Chem.—Eur. J.* **2012**, *18*, 6208−6216.

(10) Stuzhin, P. A.; Khelevina, O. G. Azaporphyrins: Structure of the Reaction Centre and Reactions of Complex Formation. *Coord. Chem. Rev.* **1996**, *147*, 41−86.

(11) *The Porphyrin Handbook*, Vol. *2*; Kadish, K. M.; Smith, R. M.; Guilard, R., Eds.; Academic Press: San Diego, 2000; pp 301−360.

(12) Matano, Y.; Fujii, D.; Shibano, T.; Furukawa, K.; Higashino, T.; Nakano, H.; Imahori, H. Covalently Linked 5,15-Diazaporphyrin Dimers: Promising Scaffolds for a Highly Conjugated Azaporphyrin Π System. *Chem.—Eur. J.* **2014**, *20*, 3342−3349.

(13) Omomo, S.; Maruyama, Y.; Furukawa, K.; Furuyama, T.; Nakano, H.; Kobayashi, N.; Matano, Y. Optical, Electrochemical, and Magnetic Properties of Pyrrole- and Thiophene-Bridged 5,15-Diazaporphyrin Dimers. *Chem.—Eur. J.* **2015**, *21*, 2003−2010.

(14) Yamamoto, M.; Takano, Y.; Matano, Y.; Stranius, K.; Tkachenko, N. V.; Lemmetyinen, H.; Imahori, H. Slow Charge Recombination and Enhanced Photoelectrochemical Properties of Diazaporphyrin-Fullerene Linked Dyad. *J. Phys. Chem. C* **2014**, *118*, 1808−1820.

(15) Chang, L. L.; Chang, C. J.; Nocera, D. G. Meso-Tetraaryl Cofacial Bisporphyrins Delivered by Suzuki Cross-Coupling. *J. Org. Chem.* **2003**, *68*, 4075−4078.

(16) Hata, H.; Yamaguchi, S.; Mori, G.; Nakazono, S.; Katoh, T.; Takatsu, K.; Hiroto, S.; Shinokubo, H.; Osuka, A. Regioselective Borylation of Porphyrins by C-H Bond Activation under Iridium Catalysis to Afford Useful Building Blocks for Porphyrin Assemblies. *Chem.—Asian J.* **2007**, *2*, 849−859.

(17) Chiu, K. Y.; Tu, Y.-J.; Lee, C.-J.; Yang, T.-F.; Lai, L.-L.; Chao, I.; Su, Y. O. Unusual Spectral and Electrochemical Properties of Azobenzene-Substituted Porphyrins. *Electrochim. Acta* **2012**, *62*, 51−62 The optical data and half-wave potentials of **P-ref** were reported. λ_Q = 550 and 587 nm in CH_2Cl_2; E_1^{ox} = +1.04 and E_1^{red} = −1.48 V vs. Ag/AgCl in CH_2Cl_2/TBAP (Fc/Fc^+ = +0.56 V)..

(18) Tkachenko, N. V.; Rantala, L.; Tauber, A. Y.; Helaja, J.; Hynninen, P. H.; Lemmetyinen, H. Photoinduced Electron Transfer in Phytochlorin−[60]Fullerene Dyads. *J. Am. Chem. Soc.* **1999**, *121*, 9378−9387.

(19) Sirbu, D.; Turta, C.; Benniston, A. C.; Abou-Chahine, F.; Lemmetyinen, H.; Tkachenko, N. V.; Wood, C.; Gibson, E. Synthesis and Properties of a *Meso*- Tris−ferrocene Appended Zinc(II) Porphyrin and a Critical Evaluation of Its Dye Sensitised Solar Cell (DSSC) Performance. *RSC Adv.* **2014**, *4*, 22733.

(20) Krishnan, R.; Binkley, J. S.; Seeger, R.; Pople, J. A. Self-Consistent Molecular Orbital Methods. XX. A Basis Set for Correlated Wave Functions. *J. Chem. Phys.* **1980**, *72*, 650.

(21) Wachters, A. J. H. Gaussian Basis Set for Molecular Wavefunctions Containing Third-Row Atoms. *J. Chem. Phys.* **1970**, *52*, 1033.

DOI: 10.1021/jp510903a
J. Phys. Chem. B 2015, 119, 7328−7337

(22) Hay, P. J. Gaussian Basis Sets for Molecular Calculations. The Representation of 3d Orbitals in Transition-Metal Atoms. *J. Chem. Phys.* **1977**, *66*, 4377.
(23) Raghavachari, K.; Trucks, G. W. Highly Correlated Systems. Excitation Energies of First Row Transition Metals Sc−Cu. *J. Chem. Phys.* **1989**, *91*, 1062.
(24) Becke, A. D. Density-Functional Thermochemistry. III. The Role of Exact Exchange. *J. Chem. Phys.* **1993**, *98*, 5648.
(25) Lee, C.; Yang, W.; Parr, R. G. Development of the Colle−Salvetti Correlation-Energy Formula into a Functional of the Electron Density. *Phys. Rev. B* **1988**, *37*, 785−789.
(26) Frisch, M.; Trucks, G.; Schlegel, H.; Scuseria, G.; Robb, M.; Cheeseman, J.; Scalmani, G.; Barone, V.; Mennucci, B.; Petersson, G.; et al. *Gaussian 09*, revision B.01.; Gaussian, Inc.: Wallingford, CT, 2009.

DOI: 10.1021/jp510903a
J. Phys. Chem. B 2015, 119, 7328−7337